# Modern techniques and Old Red problems – determining the age of continental sedimentary deposits with $^{40}Ar/^{39}Ar$ provenance analysis in west-central Norway

Elizabeth A. Eide, Nils Erik Haabesland, Per Terje Osmundsen, Torgeir B. Andersen, David Roberts & Mark A. Kendrick

Eide, E.A., Haabesland, N.E., Osmundsen, P.T., Andersen, T.B., Roberts, D. & Kendrick, M.A.: Modern techniques and Old Red problems—determining the age of continental sedimentary deposits with $^{40}Ar/^{39}Ar$ provenance analysis in west-central Norway. *Norwegian Journal of Geology,* Vol. 85, pp. 133-149. Trondheim 2005. ISSN 029-196X

Ages of continental 'Old Red Sandstone' (ORS) deposits in Norway have been notoriously difficult to obtain due to the paucity of fossil-bearing horizons. In general, $^{40}Ar/^{39}Ar$ ages from detrital mica and K-feldspar from unmetamorphosed, first-cycle sedimentary units yield *maximum* ages for sediment deposition since the detrital grains retain the ages of their crystalline basement provenance. To determine the maximum age for a presumed Lower-Middle Devonian ORS sequence in west-central Norway – the Asenøya basin – we applied $^{40}Ar/^{39}Ar$ geochronology to detrital white micas in red sandstone, and to white mica, biotite and K-feldspar from three different whole-rock clasts in an overlying conglomerate. Single-grain laser fusion of white mica from the sandstone yielded ages ranging between 416 ± 4 and 386 ± 1 Ma, with the majority of grains between ca. 400 and 392 Ma. Furnace step-heating of white mica, biotite and K-feldspar from the three rock clasts yielded weighted-mean ages of 410.2 ± 3.5 Ma, 402.7 ± 3.5 Ma and 371.0 ± 3.2 Ma, respectively. Published white mica and biotite $^{40}Ar/^{39}Ar$ cooling ages from the Central Norway basement window (CNBW), to the east and north of Asenøya, range from ca. 398 to 388 Ma; white mica and biotite $^{40}Ar/^{39}Ar$ cooling ages from the Seve and Köli Nappes, above the CNBW, range from ca. 432 to 402 Ma. Both of these primary source regions—the CNBW and the nappes—are thus represented in the red sandstone and conglomerate detritus. K-feldspar $^{40}Ar/^{39}Ar$ ages from local, CNBW basement (published age of 371 ± 8 Ma) and from orthogneiss in an offshore, *in situ* basement horst (377.3 ± 3.4 Ma, this study) further confirm the presence of appropriately-aged, proximal basement sources of CNBW type for some of the ORS conglomerate clasts. The new provenance age data demonstrate that some of the west-central Norway ORS units are younger than ca. 371 Ma—or a minimum of Late Devonian to Early Carboniferous age if time for unroofing/erosion of the basement provenance is allowed. The Asenøya sedimentary deposits are, thus, the youngest yet documented in the Norway ORS and are the last remnants of the Paleozoic sedimentary deposits of the Norwegian Caledonides that subsequently became recycled in offshore Mesozoic sedimentary basins.

*Elizabeth A. Eide, Per Terje Osmundsen & David Roberts at Geological Survey of Norway, NO-7491 Trondheim, Norway; Nils Erik Haabesland & Torgeir B. Andersen, Department of Geosciences, University of Oslo, PO Box 1047 Blindern, NO-0316 Oslo, Norway; Mark A. Kendrick, Noble Gas and $^{40}Ar$-$^{39}Ar$ Geochronology lab, The School of Earth Sciences, University of Melbourne, Victoria 3010 Australia.*

## Introduction

Fossil age constraints for continental sedimentary deposits are invariably more difficult to obtain than for marine sediments. In western Norway, where the Devonian 'Old Red Sandstone' (ORS) deposits have been key elements for addressing the late stages of tectonic development of the Scandinavian Caledonide orogen (Steel 1976; Roberts 1983; Hossack 1984; Norton 1986; Osmundsen et al. 1998; Osmundsen & Andersen 2001), precise dating of the Devonian sedimentary basins has been particularly difficult, despite pioneering work in paleontological and mapping studies since the early 20th century (e.g. Kolderup 1922; Vogt 1929; Høeg 1945). In the Hornelen, Kvamshesten and Solund basins of western Norway (Fig. 1a), plant and fish fossils were used to determine a Middle Devonian age for some of the continental clastic units (Kolderup 1922, 1926; Jarvik 1950), although well-preserved fossils and spores are relatively scarce and age determinations within and between these basins (including Håsteinen) have been made largely by stratigraphic correlation.

In the outermost Trøndelag region, sedimentary basins with fossils of latest Silurian through Mid Devonian ages have been described (Vogt 1929; Høeg 1945; Siedlecka 1975; Allen 1976) (Figs. 1a & b). A Late Silurian age was suggested by Siedlecka & Siedlecki (1972) for sedimentary rocks exposed primarily on Hitra and small islands south of Smøla; Early to Mid Devonian ages for the ORS rocks on Hitra, Ørlandet, the Storfosna islands and Tristeinen have been suggested on the basis of fossil plants and spores. Particularly critical for the latter age determinations have been the plant fossils *Psilophyton rectissimum*, *Psilophyton princeps* and *Hyenia ramosa* from Tristeinen and Ørlandet (Vogt 1929; Høeg 1945; Allen 1976).

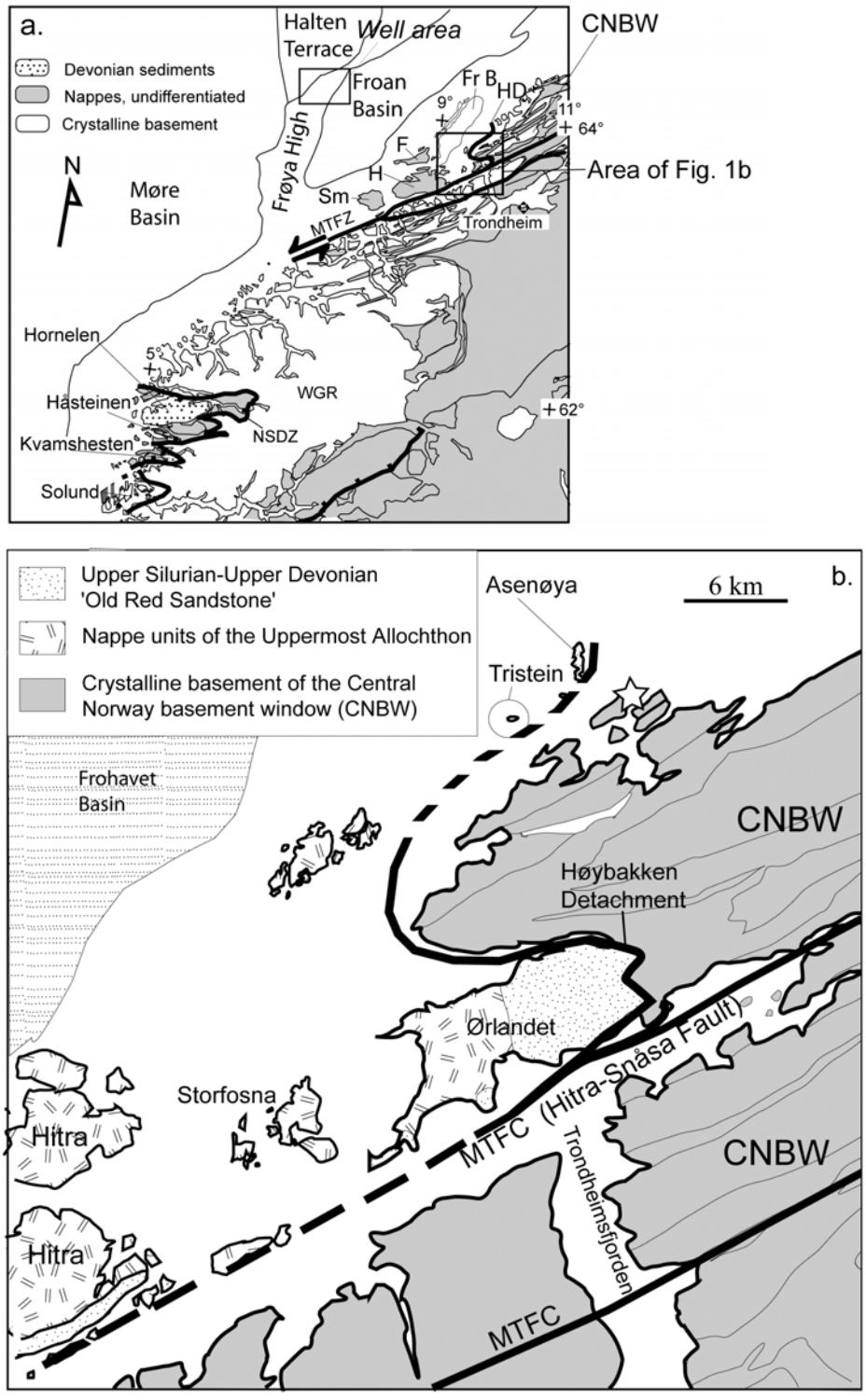


*Fig. 1: a) Geologic map of western Norway showing the position of Devonian ORS basins within the hangingwalls of regionally important, folded extensional detachments. Some primary offshore features, including the offshore well location, are indicated. The basins of western Norway (Hornelen, Håsteinen, Kvamshesten and Solund) lie within the allochthonous nappes and are juxtaposed against the Western Gneiss Region (WGR) basement culmination along the Nordfjord-Sogn Detachment Zone (NSDZ). The Siluro-Devonian sedimentary rocks of west-central Norway lie within and along the Høybakken detachment (HD) and Møre-Trøndelag Fault Complex (MTFC). The present position of the west-central Norway 'ORS' sediments is part of a hangingwall sequence also comprising allochthonous nappes. Fr B = Frohavet Basin; Sm = Smøla; H = Hitra; F = Frøya; CNBW = Central Norway basement window (cf. Braathen et al. 2000). b) Simplified geologic map of the outer Trøndelag area showing relationships between the ORS and nappe units in the hangingwall of the HD and MTFC and the CNBW. Sandstone and conglomerate units sampled for $^{40}Ar/^{39}Ar$ analysis derive from the island of Asenøya. The white star denotes the sample locality for the 371 Ma K-feldspar $^{40}Ar/^{39}Ar$ age from the study of Kendrick et al. (2004).*

Lacking their own fossil age information, the sedimentary rocks of Asenøya were presumed to be age-equivalents of the Tristeinen units, although the Asenøya rocks were probably deposited at a higher and *younger* stratigraphic level than those in the Tristeinen archipelago (Fig. 1b) (Nilsen 1972; Bøe & Sturt 1991).

All of the Devonian deposits of outermost Trøndelag and western Norway are located in the hangingwalls of regionally significant, ductile, extensional detachments capped by brittle detachment faults (e.g. Norton 1986; Séranne 1992) (Fig. 1a). $^{40}Ar/^{39}Ar$ and U/Pb dating in and around these detachments and related shear zones in western and northern Norway, combined with kinematic analysis, demonstrate that ductile shearing and basement unroofing were active during the Devonian (Fossen & Dunlap 1998; Terry et al. 2000; Eide et al. 1999, 2002; Bingen et al. 2002; Osmundsen et al. 2003; Kendrick et al. 2004) and partially overlapped in time with deposition in the tectonostratigraphically higher basins. Together, the ductile detachments and sedimentary rocks record the progressive disintegration of the Caledonide orogen, respectively, at middle and upper crustal levels. Despite their broad chronologic overlap, the evolution of and interactions between the basement substrate, the extensional detachments, and the sedimentary basins during the Devonian are not fully quantified. This is due, in part, to significant reactivation of the detachments during Late Paleozoic to Mesozoic times that has overprinted some of the Devonian fabrics (Grønlie & Torsvik 1989; Torsvik et al. 1992; Grønlie et al. 1994; Eide et al. 1997; Andersen et al. 1999; Redfield et al. 2004), to the incomplete, but growing, understanding of changes in the Devonian strain field (Séranne 1992; Watts 2001; Osmundsen et al. 2002; Braathen et al. 2002), and to lack of precise constraints on the ages of the continental sediments and related data necessary to calculate denudation and erosion/deposition rates.

As part of a regional $^{40}Ar/^{39}Ar$ and structural study to refine the late/post-collisional phase of the Paleozoic Caledonian history in Mid Norway, we sampled sedimentary rocks from the outermost exposed limit of the ORS in Norway, on the island of Asenøya (Fig. 1b & 2), and orthogneiss from an offshore crystalline basement core from an exploration well (6407/10-3) drilled through the northern end of the Frøya High (Fig. 1a). The sampled well passed through Mesozoic sediments into crystalline basement, and is, thus, an appropriate target for direct determination of the age, nature and extent of the faulted crust beneath the Late Paleozoic-Mesozoic basins. $^{40}Ar/^{39}Ar$ geochronology is a direct dating method for the offshore basement horst, but is used as an indirect dating method for unmetamorphosed clastic sediments in the ORS basin since detrital mica and K-feldspar preserve original cooling ages of their basement provenance regions.

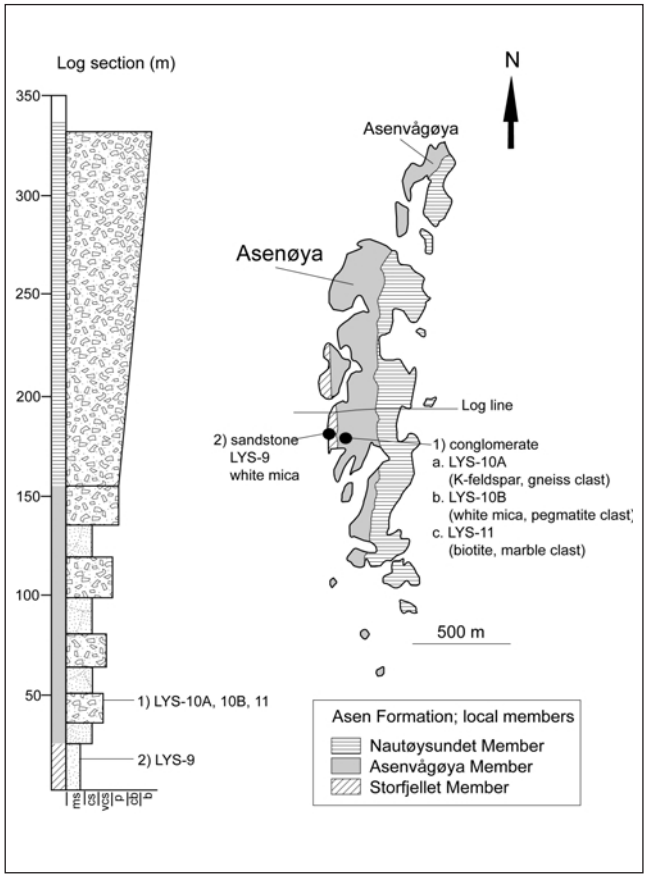


*Fig. 2: Geologic map of Asenøya and Asenvågøya with stratigraphic log. The log was measured over the section shown (Haabesland et al. 2002). Sample localities for $^{40}Ar/^{39}Ar$ analysis are indicated. ms = medium sand; cs = coarse sand; vcs = very coarse sand; p = pebble; cb = cobble; b = boulder.*

With these dating targets, our aims in this study were: 1) to obtain maximum deposition ages for ORS units otherwise lacking fossil age constraints; 2) to determine the age and type of crystalline basement that forms the Late Paleozoic-Mesozoic basin substrate along the extended Mid Norway continental margin; and 3) to use detrital and *in situ* $^{40}Ar/^{39}Ar$ ages to place minimum constraints on rates of exhumation, erosion and deposition during formation of the ORS of west-central Norway. We use the Devonian time scale of Tucker et al. (1998).

## Regional geology

In the outer Trøndelag region, Devonian clastic rocks are located in the hangingwall of the Høybakken detachment (HD), northwest of the Hitra-Snåsa branch of the Møre-Trøndelag Fault Complex (MTFC), where they are folded in open synclines about NE-SW oriented axes (Fig. 1). Combined structural analysis and $^{40}Ar/^{39}Ar$ dating in a profile from the Central Norway basement window (CNBW) upward through

*Fig. 3: a) Red sandstone from Asenøya, typical of the Storfjellet Member. Syn- and post-sedimentary faulting is clear at numerous localities. White arrow identifies pencil for scale along the bedding surface. b) Conglomerate packages typical of the Asenvågøya Member. White arrow identifies a hammer for scale.*

the Høybakken detachment indicate Early to Mid Devonian exhumation of the CNBW, associated with retrograde, top-to-the-SW extensional shearing in the HD zone and sinistral shearing along the MTFC (Kendrick et al. 2004; Osmundsen et al. submitted). Top-SW shearing occurred in concert with extension-normal shortening (Osmundsen et al. submitted). $^{40}Ar/^{39}Ar$ biotite ages of 384-381 Ma from various lithologies in the HD mylonite have been interpreted to document crystallization and cooling of the mylonite fabric during the latest phase of ductile shearing on the detachment (Kendrick et al. 2004). A brittle extensional detachment fault, the Høybakken detachment fault (HDF), subsequently decapitated the folded mylonites (Osmundsen et al. submitted).

Deposition of the Devonian sedimentary rocks is inferred to have occurred in small basins in a continental environment dominated by alluvial fans, meandering and braided rivers, floodplains and lakes (Siedlecka & Siedlecki 1972; Bøe & Sturt 1991; Haabesland et al. 2002). On Asenøya, the northernmost part of the Asen Formation preserves red-bed, alluvial-fluvial sandstones and conglomerates deposited in a half-graben dominated by west- and northwest-flowing paleocurrents (Bøe & Sturt 1991; Haabesland et al. 2002). The thickness of the Asenøya sedimentary rocks is estimated to be ca. 1.5 km and comprises, from base to top, three members of the coarsening-upward Asen Formation: the Storfjellet, Asenvågøya and Nautøysundet members (Fig. 2). The fine- to medium-grained, cross-bedded sandstones of the Storfjellet Member pass upward into alternating medium-coarse sandstones and conglomeratic sheets in the Asenvågøya Member; a prograding sequence of pebble to boulder conglomerates characterizes the uppermost, Nautøysundet Member (Haabesland et al. 2002) (Figs. 2 & 3).

On Asenvågøya, results from a detailed study of the Asenvågøya conglomerate suggested that the unit

represented part of an alluvial fan with mass flows derived from an active fault escarpment east of Asenøya (Bøe & Sturt 1991) (Fig. 1b). A fault escarpment and proximal basement source areas east-southeast of Asenøya are consistent with available data including: 1) the west and northwest paleocurrent directions; 2) the very coarse and angular (proximal) nature of some of the conglomerate sheets; and 3) some conglomerate clasts with direct correlation to basement lithologies exposed on the nearby skerries and mainland (Bøe & Sturt 1991; Haabesland et al. 2002; field observations, this study). Additionally, the sedimentary rocks on Asenøya are undeformed and unmetamorphosed, a contrast to the sedimentary rocks positioned directly above and within the HD mylonite, for example, at Ørlandet (Fig. 1), that were deformed under low-greenschist facies conditions. The undeformed and unmetamorphosed nature of the Asenøya rocks supports the proposed, initial structural position of these rocks well above the detachment (Nilsen 1972; Bøe & Sturt 1991).

The sample from the offshore exploration well (6407/10-3) comprises orthogneiss basement, unconformably overlain by a thick Lower Triassic sedimentary package, that forms part of the northern Frøya High (Fig. 1b). A strong, positive magnetic anomaly observed over the Frøya High has been attributed to a very magnetic basement source (Skilbrei et al. 2002) shown in deep-seismic interpretations as a basement high (Blystad et al. 1995). Skilbrei et al. (2002) noted similarities between the Frøya High magnetic anomaly and the strong, positive magnetic anomaly occurring over much of the CNBW and they interpreted the Frøya High as an extended piece of crystalline basement of CNBW type. As will be demonstrated below, the interpreted nature and structural position of the Frøya High basement are borne out by the $^{40}Ar/^{39}Ar$ analyses from this study.

## Sampling and analytical procedure

Measurement of Ar-isotopes in K-bearing minerals or rocks (e.g. white mica, biotite, K-feldspar, plagioclase, amphibole, whole-rock basalt) allows calculation of an age that represents the time of crystallization or cooling of the material subsequent to a metamorphic, igneous or deformation event. In provenance studies, the $^{40}Ar/^{39}Ar$ method can be applied to detrital, K-bearing mineral grains or clasts because the nominal closure temperatures at which negligible diffusion of radiogenic Ar occurs from the minerals is well above diagenetic conditions over most time-scales considered (see McDougall & Harrison 1999 for discussion). In provenance studies that employ single-grain isotope geochronology, detrital white mica is often analyzed since it is common in sandstones and siltstones and appears robust enough to survive one or more recycling episodes. In a complementary way, the minerals derived from clasts in conglomerate preserve the age-temperature history of the basement source region from which they derived and can, in some cases, be visually matched to proximal sediment supply areas. For $^{40}Ar/^{39}Ar$ analysis, minerals from conglomerate clasts can be treated in a similar way to those derived from any *in situ* basement rock, i.e. the samples can be analyzed either as pure, bulk-mineral concentrates via incremental step-heating in an oven with precise temperature control, or via single-grain laser fusion (SGLF) (one age per grain). Clearly, detrital white mica grains from sandstones must be analyzed individually (by SGLF) because each grain must, at first, be assumed to represent a unique sediment source region.

As with U/Pb detrital zircon analysis, the $^{40}Ar/^{39}Ar$ age distribution for a detrital mica population in a sandstone sample is plotted as a cumulative or relative probability distribution. The data are then compared to existing $^{40}Ar/^{39}Ar$ mica data from basement regions. This is, in a sense, 'fingerprint-matching' of detrital grain age populations to mica ages from basement. In contrast to detrial, single-grain, age-population analysis, $^{40}Ar/^{39}Ar$ furnace step-heating analyses from minerals derived from rock clasts in conglomerate can be presented in a conventional manner whereby weighted mean and inverse isochron ages are calculated and compared directly to existing $^{40}Ar/^{39}Ar$ ages from basement source regions.

On the southwest side of Asenøya, we sampled a medium-grained, cross-bedded red sandstone within the Storfjellet Member for detrital white mica (LYS-9) (Figs. 2 & 3a). Ages from these micas were obtained by SGLF. Clasts of granitic pegmatite, marble, and orthogneiss in a debris-flow conglomerate from the overlying Asenvågøya Member were sampled for white mica, biotite, and K-feldspar, respectively (LYS-10B, LYS-11, LYS-10A) (Figs. 2 & 3b). Biotite and K-feldspar concentrates from the offshore orthogneiss basement core from well 6407/10-3 were also included in the analysis; orthogneiss was collected from the 2972 m level of the well, where 15 m of basement had been penetrated. The mica and K-feldspar concentrates from the conglomerate clasts and the offshore core were analyzed by resistance-furnace step-heating. Laser and furnace analyses were conducted in the $^{40}Ar/^{39}Ar$ geochronology laboratory at the Geological Survey of Norway (NGU). Analytical protocol is presented in the appendix and otherwise follows Eide et al. (2002). Data descriptions refer to Figure 4; the data are presented in Table 1 and are summarized in Table 2. All ages obtained in this study are cited at $1\sigma$ including a J-value uncertainty of 1%.

## Results

K-feldspar from the northern Frøya High well (6407/10-3 orthogneiss) showed reasonably consistent gas release over the majority of the furnace step-heating experiment. The apparent ages for the initial eleven, low-temperature, low-volume steps increase from ca. 308 to 384 Ma; the remainder of the spectrum, comprising ca. 91% of the cumulative gas, yields a weighted-mean age of 377.3 ± 3.4 Ma for a series of relatively concordant steps (Fig. 4a; Tables 1 & 2). The inverse isochron for the feldspar was not illuminating due to the very radiogenic nature of a majority of the steps in the near-plateau. The biotite spectrum from the same sample yields a somewhat irregular apparent age pattern with a range between ca. 403 and 384 Ma (Table 1). An inverse isochron through the high-temperature, high gas-volume steps of the experiment yields a poor fit of a line to the data corresponding to an age of 394.4 ± 3.9 Ma with a poorly constrained upper intercept (Fig. 4b); a wide spread of the most radiogenic data points along the x-axis intercept contributes to this uncertainty. A non-atmospheric trapped argon component may account for some of the irregularity (and older apparent ages) observed in the biotite release spectrum, although this is not precisely constrained with the present data set (Fig. 4b; Tables 1 & 2).

Most of the gas for white mica LYS-10B (pegmatite clast, conglomerate) was released in five nearly concordant steps. A weighted mean age of these steps (98.7% of cumulative $^{39}Ar$ gas) is 410.2 ± 3.5 Ma. The same steps on an isochron define a linear array with an age of 410.4 ± 3.6 Ma and a trapped argon component of atmospheric value (Fig. 4a,c; Tables 1 & 2). The fit of a line to the data is slightly greater than statistically acceptable (SUMS/n-2 = 4.1, or greater than the F-variate critical value, see Table 2), largely due to the small uncertainties on individual data points.

The release spectrum for biotite LYS-11 (marble clast, conglomerate) yielded a set of nearly concordant steps with a weighted mean age of 402.7 ± 3.5 Ma over 90.5% of the cumulative gas released in the experiment (Fig. 4a). An inverse isochron of the same steps yielded an age within uncertainty of the spectrum age, but with poor constraint on the upper intercept due to the radiogenic nature of the steps used in the regression (Table 2).

The release spectrum for K-feldspar (LYS-10A) from the orthogneiss clast yielded an initial set of six, low-temperature, low-volume steps with apparent ages ranging between 346 Ma and 384 Ma. The remainder of the experiment, comprising ca. 85% of the gas released, contains a set of semi-concordant steps with a weighted-mean age of 371.0 ± 3.2 Ma (Fig. 4a; Tables 1 & 2). On an inverse isochron, the same data define a reasonably linear array, albeit with poor fit of the line to the data (Fig. 4d). The lower intercept corresponds to an age of 370.3 ± 3.9 Ma with a trapped, near-atmospheric $^{40}Ar/^{36}Ar$ ratio of 293.6 ± 29.3 (Tables 1 & 2).

Single-grain laser fusion of 26 detrital white mica grains from the Asenøya red sandstone (LYS-9) yielded ages between 416 ± 4 Ma and 386 ± 1 Ma (Tables 1 & 2). A cumulative probability distribution of these data indicates that the majority of the high-precision single-grain ages vary between ca. 400 and 392 Ma, i.e. latest Early- early Mid Devonian (Eifelian) (Fig. 4e).

## $^{40}Ar/^{39}Ar$ data interpretation

The weighted-mean ages calculated for the most concordant parts of the release spectra for white mica LYS-10B, biotite LYS-11 and K-feldspar LYS-10A from the three conglomerate clasts statistically overlap with lower intercept ages derived from their respective inverse isochrons. This statistical similarity, the relatively consistent gas-release patterns, and the trapped argon components of atmospheric value support interpretation of the ages 410.2 ± 3.5, 402.7 ± 3.5 and 371.0 ± 3.2 Ma, respectively, as preserved, syn-to-post collisional cooling ages of the original pegmatite, marble and orthogneiss basement units that sourced these clasts. Similar reasoning holds with regard to the K-feldspar data from the offshore, *in situ* basement core and the age of 377.3 ± 3.4 Ma is interpreted as a cooling age related to the time that this mineral began to retain radiogenic argon. Biotite from the same offshore orthogneiss had an irregular release spectrum and we interpret the ca. 394 ± 4 Ma inverse isochron age as a maximum cooling age for the basement unit through a temperature range appropriate for argon retention in the biotite. The ages for the two K-feldspars overlap within uncertainty and can be said to have closed to argon diffusion at a statistically similar time in the Late Devonian. While no precise argon closure temperatures are calculated for the minerals analyzed in this study, the younger ages of K-feldspar relative to mica are consistent with a slightly higher, relative closure temperature for biotite and white mica (ca. 300-400°C), compared to K-feldspar (ca. 250°C) (see McDougall & Harrison 1999 for discussion).

Since the red sandstone is undeformed and unmetamorphosed, the detrital, single-grain white mica ages from the Asenøya unit are interpreted to represent preserved cooling ages of different metamorphic source regions in the CNBW and Caledonian nappes (see also below). The detritus from the sandstone is, thus, assumed to have derived from crystalline white mica-bearing units with cooling ages ranging between ca. 416 and 386 Ma.

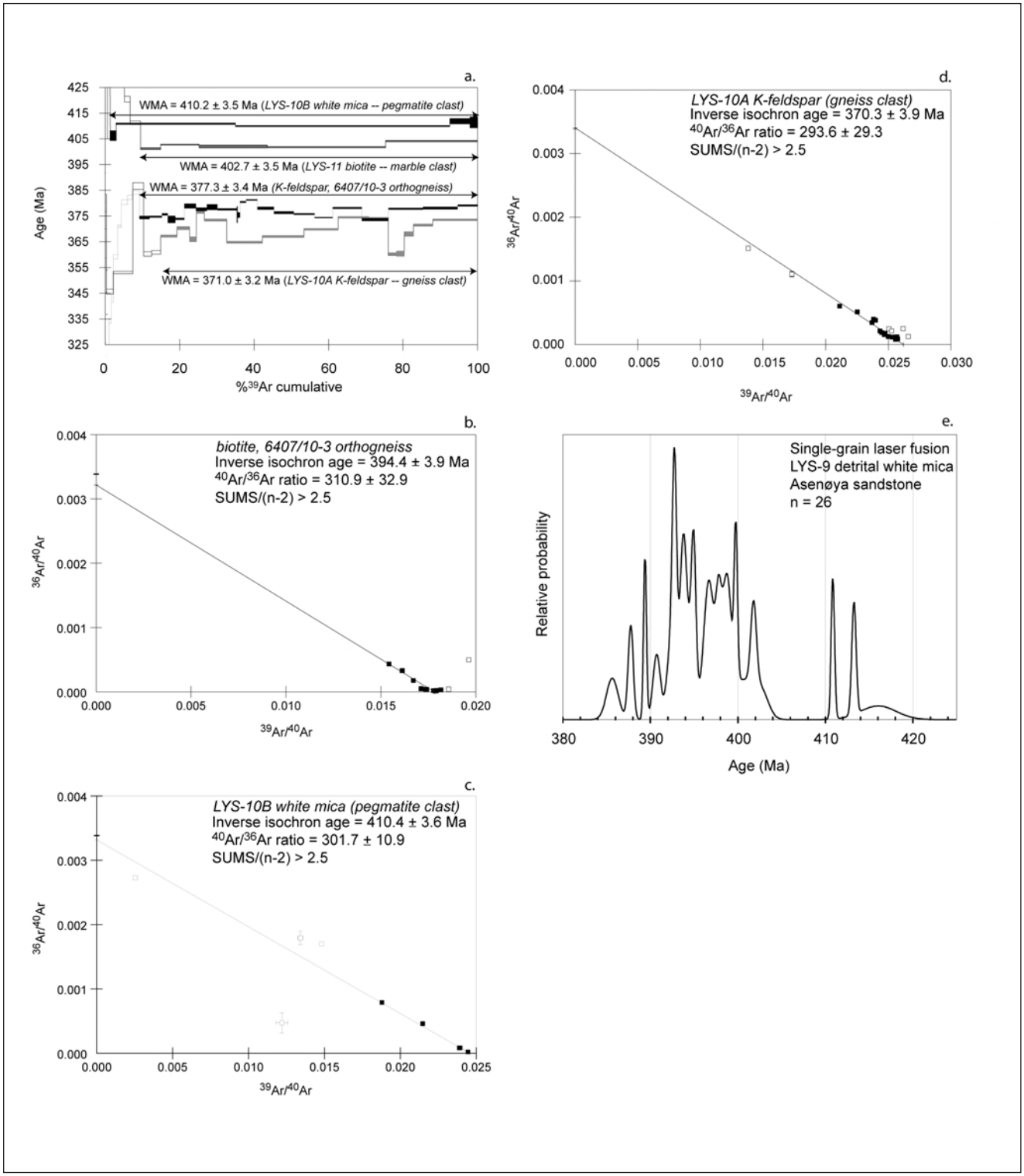


*Fig. 4: a) $^{40}Ar/^{39}Ar$ release spectra from resistance-furnace step-heating of white mica, biotite and K-feldspar from three conglomerate clasts and K-feldspar from the offshore orthogneiss basement core (exploration well 6407/10-3). Ages are weighted mean ages (WMA) calculated over the indicated portions of the spectra. b) Inverse isochron for biotite from the offshore orthogneiss basement core; very poor fit of a line to the data is largely due to the wide spread of the most radiogenic data points along the x-axis. Irregularity of the release spectrum for this sample suggests complications from non-atmospheric trapped argon components. The isochron age is interpreted as an imprecise maximum age for the cooling of the biotite from the rock. c) Inverse isochron for white mica from the granitic pegmatite clast LYS-10B (release spectrum shown in (a)). The isochron age overlaps the weighted mean age within uncertainty and the upper intercept indicates an atmospheric trapped argon component. d) Inverse isochron for K-feldspar from the gneiss clast LYS-10A (release spectrum shown in (a)). The isochron age overlaps the weighted mean age within uncertainty and the upper intercept indicates an atmospheric trapped argon component. e) Relative probability plot of 26 detrital white mica ages from sandstone LYS-9; ages were derived by single-grain laser fusion.*

## Discussion

*Age of the sedimentary rocks of the Asen Formation*

Neither the red sandstone nor the conglomerate from Asenøya appears to have surpassed diagenetic conditions and we exclude the possibility that the ages from the detrital micas or the feldspar in the Asen Formation were reset subsequent to deposition. This allows a straightforward interpretation of the provenance age data and we conclude that the sedimentary rocks on Asenøya must be younger than the $^{40}Ar/^{39}Ar$ cooling ages of their constituent detritus: the Storfjellet Member must be younger than the youngest detrital white mica age of 386 ± 1 Ma (Givetian) and the Asenvågøya Member must be Famennian or younger (younger than the 371.0 ± 3.2 Ma K-feldspar age) (Fig. 5). The age for the Asen Formation was previously interpreted as Early to Middle Devonian based on correlation with the rocks containing plant fossils and spores on Tristeinen and Ørlandet (cf. Allen 1976). The new $^{40}Ar/^{39}Ar$ detrital ages supercede that correlation and indicate that some of the sedimentary rocks on Asenøya are at least latest Devonian to perhaps Early Carboniferous in age, if time for unroofing and erosion of basement source areas and subsequent transport and deposition is allowed.

Our interpretation of the Asen Formation as Late Devonian to Early Carboniferous in age concurs with that of Nilsen (1972) and Bøe & Sturt (1991) who suggested that the ORS deposits on Asenøya and nearby islands were part of a different Devonian basin of 'younger' age than those exposed on the mainland (Ørlandet), and on Storfosna and Hitra (Fig. 1a, b). Our new data confirm that the sedimentary rocks exposed on Asenøya constitute the youngest preserved Paleozoic sedimentary rocks so far reported from western Norway.

*Provenance for detrital mica and conglomerate clasts*

Provenance data, whether biostratigraphic, or of bulk-rock, heavy-mineral or single-grain isotope nature (U/Pb zircon or $^{40}Ar/^{39}Ar$ mica and feldspar), are usually used to assess the type and location of crustal source(s) supplying sediment to a depocenter, and can, thus, facilitate interpretation of sediment pathways and dispersal patterns (see Morton 1996 for review). In the absence of data to the contrary, provenance studies generally make two initial, simplifying assumptions: 1) the source regions (basement ± basins) that supplied sediment to the depocenter are still present and accessible; 2) basement areas considered to be potential sediment source regions were not covered at the time of erosion, transport and deposition of the studied sediment. These assumptions and interpretation of the provenance data require modification if the sedimentary units under investigation are recycled and/or if a comparable database from the potential source regions is not available.

While provenance data rarely yield unique 'fingerprint' identification of an exact basement source that supplied a specific sedimentary sequence, knowledge of the structural evolution of the area and an appropriate database to which provenance data can be compared will naturally reduce uncertainties in interpretation of potential source regions. With regard to reducing this uncertainty, single-grain isotope geochronology provenance methods (U/Pb or $^{40}Ar/^{39}Ar$) have particular advantages in areas like the Caledonides where high-precision ages from a fairly large areal distribution of exposed basement regions (that could have supplied sediment to the sediment packages) are available in the public domain. The specific, relatively ordered and well-dated history of basement crystallization, nappe emplacement and post-metamorphic/post-deformation cooling associated with the Caledonian orogeny allows fairly distinct basement and nappe source regions to be distinguished: the $^{40}Ar/^{39}Ar$ age compilation for Mid Norway, Nordland and the Caledonide area of Mid Sweden in Figure 5 derives from numerous published studies, most of which are summarized in Eide & Solli (2002), and serves as the template against which detrital mica and K-feldspar ages were compared in this study.

The provenance data indicate that both nappe and crystalline CNBW basement units sourced the Asenøya basin from the east and south. The proximal nature of the Asenøya conglomerate supports a nearby basement source region of CNBW type for the orthogneiss clast (K-feldspar age, Fig. 5). The gneiss clast K-feldspar (LYS-10A) age of 371.0 ± 3.2 Ma overlaps exactly with the K-feldspar age (371 ± 8 Ma, 2s) from CNBW basement dated immediately below the HD (Figs. 1b, 5; Kendrick et al. 2004). Additionally, the similarity between K-feldspar ages from the offshore Frøya High sample in this study (377.3 ± 3.4 Ma) and the CNBW basement below the HD (Kendrick et al. 2004) lends further support to geophysical interpretations that the basement of the CNBW and the Frøya High are of similar character and were part of the same crustal package, prior to latest Paleozoic-Mesozoic rifting (Skilbrei et al. 2002; Osmundsen et al. 2002).

Based upon age 'fingerprints' (Fig. 5), the source region for the pegmatite clast LYS-10B (white mica age of 410.2 ± 3.5 Ma) was most likely a nappe unit. Toward the east and south of the CNBW, Köli Nappe white mica ages range between ca. 425 and 402 Ma (Dallmeyer et al. 1985; Hacker & Gans in press), while the oldest published white mica age from the CNBW is 395 ± 2 Ma (Dallmeyer et al. 1992). Relative to Asenøya, nappe units are presently exposed to the northeast, above the Kollstraumen detachment, to the south above the HD,

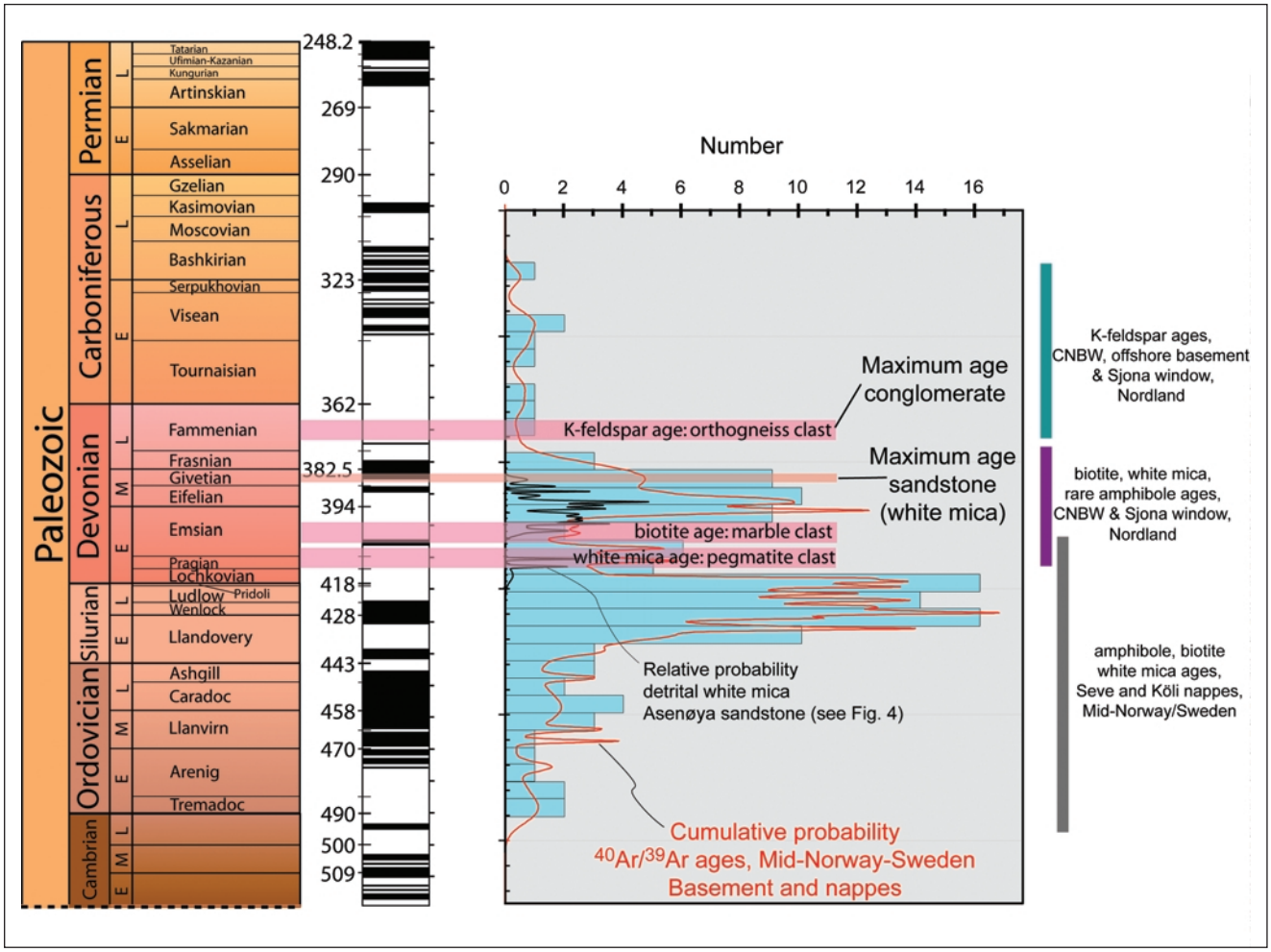


*Fig. 5: Left: Paleozoic time scale and geomagnetic polarity time scale (GPTS) (after compilation in Eide 2002); hachures on the right side of the GPTS are every 10 m.y. Right: Cumulative probability distribution of published $^{40}Ar/^{39}Ar$ ages for Mid Norway/Sweden (blue histogram with red probability overlay); corresponding minerals and tectonostratigraphic units are noted to the far right and derive from the compilation of Eide & Solli (2002). The only addition to the data compilation from the latter study is the recently published work of Kendrick et al. (2004). The relative probability distribution from Figure 4 for white mica from the sandstone of the Storfjellet Member (black probability distribution) is overlain on the cumulative probability distribution for Mid Norway/Sweden basement and nappes to 'fingerprint' the provenance of the detrital grains. Close correspondence between the detrital white mica peak and the white mica-dominated age peak from the CNBW basement units is clear. Maximum age for the sandstone is indicated by the youngest white mica in its population (386 ± 1 Ma); a maximum age for the conglomerate is indicated by the youngest clast, identified as a 371.0 ± 3.2 Ma K-feldspar (LYS-10A). The latter has direct provenance from the underlying orthogneiss basement of the CNBW (K-feldspar, Kendrick et al. 2004) and the offshore Frøya High (K-feldspar, this study).*

and eastward on the Fosen peninsula, along the MTFC and into Sweden (Figs. 1 & 5). While the presence of nappe units located today relatively far from the Asenøya basin may appear to belie the proximal nature of the conglomerate clasts in Asenøya, we suggest that proximal nappe units of Seve-Köli type and age did exist and may have supplied the clast to the Asenøya conglomerate, but these units are presently not locally exposed, having been either eroded or concealed.

While marble lithologies are found within the mylonite of the HD, these units are unlikely to be the source for the marble clast (LYS-11) dated in this study (biotite age of 402.7 ± 3.5 Ma): the $^{40}Ar/^{39}Ar$ biotite age from a local HD marble is 381 ± 6 Ma (Kendrick et al. 2004) and U/Pb titanite ages from similar supracrustal units near the HD range from 405 to 399 Ma (Bingen et al. 2002), indicating that the marble clast in this study is older than these local varieties. The only biotite from the CNBW with a $^{40}Ar/^{39}Ar$ age (395 ± 1 Ma) similar to the biotite age from the marble clast was reported from the core of the CNBW, about 100-120 km north and east of Asenøya (Dallmeyer et al. 1992), but the biotite derives from a different rock type (mica schist). Because of the proximal nature of the conglomerate and the age of the marble clast, we suggest, therefore, that the most likely source for this clast was a proximal nappe unit of Seve or Köli type that is presently not exposed. Seve and Köli nappes both contain marble lithologies elsewhere in the Caledonides.

The detrital white mica ages from the red sandstone of the Storfjellet Member on Asenøya indicate derivation of the grains primarily from the metamorphic basement of the CNBW, with a smaller contribution from Caledonian nappe units (Fig. 5). Dallmeyer et al. (1992) reported $^{40}Ar/^{39}Ar$ ages for white mica of ca. 395-390 Ma from the northeastern CNBW (denoted the 'Vestranden gneiss complex'); Kendrick et al. (2004) reported two white mica ages from the footwall HD mylonite and nearby, underlying CNBW basement of 383 ± 6 and 387 ± 6 Ma (2σ), respectively. These CNBW and HD mylonite ages overlap with the primary sample group in our detrital mica population (Fig. 5; Table 1). The nappes north and east of Trondheim, toward Sweden, generally yield white mica ages older than 405 Ma (Dallmeyer et al. 1985; Hacker & Gans in press), and could have served as sources for the few, older mica ages in our dataset. Alluvial fan systems supplying the sandstone sediment to the basin could have sampled both primary rock types, CNBW and nappes, over transport distances that were likely greater than those for the overlying conglomerate.

On balance, the provenance data could be used to infer a slight change in source region between deposition of the Storfjellet and Asenvågøya members. The data indicate a predominantly CNBW source for the Storfjellet Member sandstone, while a more mixed CNBW + nappe source area is implied for the Asenvågøya Member conglomerate. We note, however, that the clast sample age population from the conglomerate should be supplemented to add confidence to any inferred shift in source region supplying these two members.

### *Quantifying unroofing and erosion rates and timing of regional deformation*

Adopting a conservative range of K-feldspar Ar-closure temperatures of ca. 200-300°C, we can presume that the gneiss basement corresponding to the conglomerate clast LYS-10A was at a depth between 8 and 15 km at 371 Ma (appropriate for an average to slightly cool geothermal gradient of ~20-25°C/km). From such depths, the exhumation, exposure, and erosion of the CNBW basement and eventual deposition of the 371 Ma gneiss clast into the Asenøya basin *before* the end of Devonian time (362 Ma) would not require abnormally high exhumation rates: ~0.8-1.5 mm/yr would suffice, if constant rates are assumed and erosion balances exhumation. Should the units of the Asen Formation exposed on Asenøya have been deposited in Early Carboniferous time, slower rates could well apply. Our data accord with those of previous workers who suggested that much of the exhumation of the deep crust (Western Gneiss Region (WGR) and CNBW equivalents) had already been completed when the Devonian basins formed and that unroofing rates had slowed by ca. 395 Ma (Terry et al. 2000; Dallmeyer et al. 1992; Kendrick et al. 2004).

In the Hornelen basin, clast population analysis in conglomerate indicated primary derivation of the sediments from the nappes and not from the high-grade, metamorphic WGR; this interpretation was based in large part on the lack of eclogite or other high-pressure metamorphic clasts in the Hornelen sedimentary units (Cuthbert 1991). Recent work using detrital zircon and whole-rock Sm-Nd analysis (Fonneland 2002) has indicated that some WGR contribution to the Hornelen sediments may also be present in Hornelen sedimentary units, although this contribution was probably subordinate to sediment derived from the nappes. In keeping with a scenario of progressive exhumation of the basement substrate, the 'younger' ORS from Asenøya would be expected to have derived detritus from yet deeper levels of the tectonostratigraphy. This appears to be borne out with the provenance data in this study that indicate significant sediment contributions from well within the CNBW basement, in addition to some contribution from the nappe units.

As is the case with the Devonian basins of western Norway (Fig. 1a), the Siluro-Devonian basins of the outer Trøndelag region have a well-documented deformation fabric suggested to be of Late Devonian age and possibly related to the 'Svalbardian' tectonic event (Vogt 1929; Holtedahl 1960; Roberts 1981, 1983). 'Svalbardian' initially referred to Late Devonian-Early Carboniferous deformation on Svalbard and Bjørnøya where folded Devonian sediments are overlain by flat-lying Carboniferous red beds (Vogt 1929). This designation was later extended to include the folded Devonian sediments of western Norway (e.g. Holtedahl 1960; Roberts 1983) where paleomagnetic and $^{40}Ar/^{39}Ar$ studies on the fault fabrics and basement have provided more precise Late Devonian-Early Carboniferous age constraints for the latest phase of deformation and unroofing (Torsvik et al. 1986; Eide et al. 1999). Nilsen (1972) proposed a scenario whereby the 'Svalbardian' episode probably incorporated "syndepositional graben formation, repeated uplift of source areas, and tectonic movements" and our new results concur with this general idea. We note that studies within the sedimentary basins of western Norway suggest that folding commenced already during Middle Devonian sedimentation (Chauvet & Séranne 1994; Osmundsen et al. 2000); deformation then continued through at least Late Devonian-Early Carboniferous time.

### *Implications for sedimentary recycling*

Because the $^{40}Ar/^{39}Ar$ method records ages sensitive to changes in tectonostratigraphic level, a detailed provenance program in the Devonian basins could aid in

refining the lithostratigraphy, age and depositional sequence of different parts of the ORS along the coast of Norway. This type of information would also be important in the light of recent provenance studies offshore Norway (Sherlock 2001; Bugge et al. 2002) and in East Greenland (Hartz et al. 2002; Whitham et al. 2004), which suggested that contributions to Mesozoic sedimentary packages may have come both from erosion of crystalline basement source regions as well as from recycling of sedimentary rocks in Late Paleozoic basins. The proximity of the Jurassic Frohavet Basin to the ORS basin remnants of Mid Norway (Fig. 1; Sommaruga & Bøe 2002) and the absence of Upper Paleozoic sedimentary units onshore would suggest that the Jurassic sequences contain some proportion of recycled, sediment from the Mid Norway Paleozoic basins. In their analysis of the Upper Permian-Lower Triassic sedimentary units of the Helgeland Basin, Bugge et al. (2002) speculated that red-colored, Upper Devonian-Lower Permian sedimentary units probably served as the main provenance for the reddish, recycled detritus in an Upper Permian shallow-marine sequence. Recent apatite fission-track analyses across strands of the MTFC (Redfield et al. 2004) have yielded cooling histories interpreted to document discrete, Mesozoic block uplift patterns that may tie directly to episodes of recycling of some of this later Paleozoic sedimentary package. The results from the present study demonstrate that the Asenøya sedimentary deposits are not only the youngest yet documented in the Norway 'ORS', but are also the last remnants of the Paleozoic sedimentary deposits of the Norwegian Caledonides that subsequently became recycled in latest Paleozoic and Mesozoic sedimentary basins.

## Conclusions

Given the occurrence of complete Upper Paleozoic sedimentary packages on East Greenland, Svalbard and Bjørnøya, the presence of small vestiges of ORS deposits in western Norway that are at least of Late Devonian age, as identified here, is not surprising. This study's importance rather lies in the demonstrated potential for the $^{40}Ar/^{39}Ar$ geochronology method to be used as an effective tool to perform indirect dating of clastic sediments where appropriate fossils are absent or poorly preserved, to supply data to test geophysical interpretations of onshore and offshore basement correlations, and to aid in quantification of the rates of geological processes associated with exhumation and basin sedimentation.

*Acknowledgements:* The samples and data acquired in this study were primarily obtained under the auspices of the BAT project, a cooperative, super-endeavor between the Geological Survey of Norway and Conoco-Phillips, ExxonMobil, Statoil, Shell, Norsk Agip, BP, Norsk Hydro and ChevronTexaco during the years 1998-2002.

## References

Allen, K.C. 1976: Devonian spores from outer Trøndelag, Norway. *Norsk Geologisk Tidsskrift 56*, 437-448.

Andersen, T.B., Torsvik, T.H., Eide, E.A., Faleide, J.I. & Osmundsen, P.T. 1999: Permian and Mesozoic faulting in central South Norway. *Journal of the Geological Society, London 156*, 1073-1080.

Bingen, B., Nordgulen, Ø. & Solli, A. 2002: Field, laboratory and theory: application of the datasets to the Mid Norway setting. D. U-Pb geochronology of Paleozoic events in the Mid Scandinavian Caledonides. *In* Eide, E.A. (coord.), *BATLAS – Mid Norway plate reconstruction atlas with global and Atlantic perspectives.* Geological Survey of Norway, 66-67.

Blystad, P., Brekke, H., Færseth, R.B., Larsen, B.T., Skogseid, J. & Tørudbakken, B. 1995: Structural elements of the Norwegian continental shelf, Part 2. The Norwegian Sea Region. *Norwegian Petroleum Directorate Bulletin 8*, 45pp., 17 figures.

Braathen, A., Nordgulen, Ø., Osmundsen, P.-T., Andersen, T.B., Solli, A. & Roberts, D. 2000: Devonian, orogen-parallel, opposed extension in the Central Norwegian Caledonides. *Geology 28*, 615-618.

Braathen, A., Osmundsen, P.T., Nordgulen, Ø., Roberts, D. & Meyer, G.B. 2002: Orogen-parallel extension of the Caledonides in northern Central Norway: an overview. *Norwegian Journal of Geology 82*, 225-241.

Bugge, T., Ringås, J.E., Leith, D.A., Mangerud, G., Weiss, H.M. & Leith, T.L. 2002: Upper Permian as a new play model on the mid-Norwegian continental shelf – Investigated by shallow stratigraphic drilling. *AAPG Bulletin 86*, 107-127.

Bøe, R. & Sturt, B.A. 1991: Textural responses to evolving mass-flows: an example from the Devonian Asen Formation, central Norway. *Geological Magazine 128*, 99-109.

Chauvet, A. & Sèranne, M. 1994: Extension-parallel folding in the Scandinavian Caledonides: implications for late-orogenic processes. *Tectonophysics 238*, 31-54.

Cuthbert, S.J. 1991: Evolution of the Devonian Hornelen Basin, west Norway: new constraints from petrological studies of metamorphic clasts. *In* Morton, A.C., Todd, S.P & Haughton, P.D.W. (eds.), *Developments in Sedimentary Provenance Studies.* Geological Society of London, Special Publications 57, 343-360.

Dallmeyer, R.D., Gee, D.G. & Beckholmen, M. 1985: $^{40}Ar/^{39}Ar$ mineral age record of early Caledonian tectonothermal activity in the Baltoscandian miogeocline, central Scandinavia. *American Journal of Science 285*, 532-568.

Dallmeyer, R.D., Johansson, L. & Möller, C. 1992: Chronology of Caledonian high-pressure granulite-facies metamorphism, uplift, and deformation within northern parts of the Western Gneiss Region, Norway. *Geological Society of America Bulletin 104*, 444-455.

Dalrymple, G.B., Alexander, E.C., Lanphere, M.A., & Kraker, G.P. 1981: Irradiation of samples for $^{40}Ar/^{39}Ar$ dating using the Geological Survey TRIGA reactor. *Geological Survey Professional Paper 1176*, 1-55.

Duffield,W.A. & Dalrymple, G.B. 1990: The Taylor Creek Rhyolite of New Mexico; a rapidly emplaced field of lava domes and flows. *Bulletin of Volcanology 52*, 475-487.

Eide, E.A. 2002: Introduction – Plate reconstructions and integrated datasets. *In* Eide, E.A. (coord.), *BATLAS – Mid Norway plate reconstruction atlas with global and Atlantic perspectives.* Geological Survey of Norway, 18-39.

Eide, E.A. & Solli, A. 2002: Field, laboratory and theory: application of the datasets to the Mid Norway setting. E. $^{40}Ar/^{39}Ar$ geochronology of Paleozoic events in the Mid Scandinavian Caledonides. *In* Eide, E.A. (coord.), *BATLAS – Mid Norway plate reconstruction atlas with global and Atlantic perspectives*. Geological Survey of Norway, 68-69.

Eide, E.A., Torsvik, T.H. & Andersen, T.B. 1997: Absolute dating of brittle fault movements: Late Permian and Late Jurassic extensional fault breccias in western Norway. *Terra Nova 9*, 135-139.

Eide, E.A., Torsvik, T.H., Andersen, T.B. & Arnaud, N. O. 1999: Early Carboniferous unroofing in western Norway: A tale of alkali feldspar thermochronology. *Journal of Geology 107*, 353-374.

Eide, E.A., Osmundsen, P.T., Meyer, G.B., Kendrick, M.A. & Corfu, F. 2002: The Nesna Shear Zone, north-central Norway: an $^{40}Ar/^{39}Ar$ record of Early Devonian-Early Carboniferous ductile extension and unroofing. *Norwegian Journal of Geology 82*, 317-339.

Fonneland, H.C. 2002: Radiogenic isotope systematics of clastic sedimentary rocks; with emphasis on detrital zircon geochronology. Unpublished doctoral dissertation. University of Bergen. 102 pp.

Fossen, H. & Dunlap, W.J. 1998: Timing and kinematics of Caledonian thrusting and extensional collapse, southern Norway: evidence from 40Ar/39Ar thermochronology. *Journal of Structural Geology 20*, 765-781.

Grønlie, A. & Torsvik, T.H. 1989: On the origin and age of hydrothermal thorium enriched carbonate veins and breccias in the Møre-Trøndelag Fault Zone, central Norway. *Norsk Geologisk Tidsskrift 69*, 1-19.

Grønlie, A., Naeser, C.W., Naeser, N.D., Mitchell, J.G., Sturt, B.A. & Ineson, P. 1994: Fission track and K/Ar dating of tectonic activity in a transect across the Møre-Trøndelag Fault Zone, Central Norway. *Norsk Geologisk Tidsskrift 74*, 24-34.

Hacker, B.R. & Gans, P.B. in press: Creation of ultrahigh-pressure terranes: Petrology and thermochronology of nappes in the central Scandinavian Caledonides. *Geological Society of America Bulletin.*

Hartz, E.H., Eide, E.A., Andresen, A., Midbøe, P. & Hodges, K.V. 2002: Detrital feedback on basin models: $^{40}Ar/^{39}Ar$ white mica geochronology applied to the Hold With Hope profile, East Greenland. *Norwegian Journal of Geology 82*, 341-358.

Holtedahl, O. 1960: Devonian. Including Downtonian in the Hitra district. *Norges geologiske undersøkelse 208*, 285-297.

Hossack, J.R. 1984: The geometry of listric normal faults in the Devonian basins of Sunnfjord, W. Norway. *Journal of the Geological Society, London 141*, 629-637.

Høeg, O.A. 1945: Contributions to the Devonian flora of western Norway. III. *Norsk Geologisk Tidsskrift 25*, 183-198.

Haabesland, N.E., Osmundsen, P.-T. & Andersen, T.B. 2002: Tectonosedimentary evolution of the Asen Formation, in a Devonian half-graben at Fosen, Trøndelag. *Norsk Petroleum Forening Abstracts and Proceedings 2*, 100-103.

Jarvik, E. 1950: On the Middle Devonian Crossopterygians from the Hornelen field in western Norway. *Bergens Museum Aarbok. 1948, Naturvitenskaps række 8*. 48 pp.

Kendrick, M.A., Eide, E.A., Roberts, D. & Osmundsen, P.T. 2004: The Middle to Late Devonian Høybakken detachment, central Norway: $^{40}Ar/^{39}Ar$ evidence for prolonged late/post-Scandian extension and uplift. *Geological Magazine 141*, 329-344.

Kolderup, C.F. 1922: Kvamshestens devonfelt. *Bergens Museum Aarbok. 1920-21, Naturvitenskaps række 4*. 96 pp.

Kolderup, C.F. 1926: Solunds devonfelt. *Bergens Museum Aarbok. 1924-25, Naturvitenskaps række 8*. 73 pp.

McDougall, I. & Harrison, T.M. 1999: *Geochronology and Thermochronology by the $^{40}Ar/^{39}Ar$ Method*. Oxford University Press, Oxford.

Morton, A.C. 1996: Geochemical studies of detrital heavy minerals and their application to provenance research. *In* Morton, A.C., Todd, S.P. & Haughton, P.D.W. (eds.), *Developments in Sedimentary Provenance Studies*. Geological Society Special Publication 57, 31-45.

Nilsen, T.H. 1972: Devonian (Old Red Sandstone) sedimentation and tectonics of Norway. *Arctic Geology, American Association of Petroleum Geologists Memoir 19*, 471-481.

Norton, M.G. 1986: Late Caledonian extension in western Norway: a response to extreme crustal thickening. *Tectonics 5*, 195-204.

Osmundsen, P.T. & Andersen, T.B. 2001: The Middle Devonian basins of western Norway; sedimentary response to large-scale transtensional tectonics? *Tectonophysics 332*, 51-68.

Osmundsen, P.T., Andersen, T.B., Markussen, S. and Svendby, A.K. 1998: Tectonics and sedimentation in the hangingwall of a major extensional detachment: the Devonian Kvamshesten Basin, western Norway. *Basin Research 10*, 213-234.

Osmundsen, P.T., Bakke, B.A., Svendby, A.K. & Andersen, T.B. 2000: Architecture of the Middle Devonian Kvamshesten Group, western Norway: sedimentary response to deformation above a ramp-flat extensional fault. *In* Friend, P.D. & Williams, B.P.J. (eds), *New Perspectives on the Old Red Sandstone*. Geological Society, London, Special Publications 180, 503-535.

Osmundsen, P.T., Sommaruga, A., Skilbrei, J.R. & Olesen, O. 2002: Deep structure of the Norwegian Sea area, NE Atlantic margin. *Norwegian Journal of Geology 82*, 205-224.

Osmundsen, P.T., Braathen, A., Nordgulen, Ø., Roberts, D., Meyer, G.B. & Eide, E.A. 2003: The Devonian Nesna Shear Zone and adjacent gneiss-cored culminations, north-central Norwegian Caledonides. *Journal of the Geological Society, London 160*, 137-150.

Redfield, T.F., Torsvik, T.H., Andriessen, P.A.M. & Gabrielsen, R.H. 2004: Mesozoic and Cenozoic tectonics of the Møre-Trøndelag Fault Complex, central Norway: constraints from new apatite fission track data. *Physics and Chemistry of the Earth 29*, 673-682.

Rex, D.C. & Guise, P.G. 1995: Evaluation of argon standards with special emphasis on time scale measurements. *In* Odin, G.S. (ed.): *Phanerozoic Time Scale. Bulletin Liassic Information. IUGS Subcommission on Geochronology 13*, 21-23.

Roberts, D. 1981: Some features of tectonic deformation of Old Red Sandstone sediments on Hitra, West Central Norway. *Norges geologiske undesøkelse 370*, 45-48.

Roberts, D. 1983: Devonian tectonic deformation in the Norwegian Caledonides and its regional perspectives. *Norges geologiske undersøkelse 380*, 85-96.

Séranne, M. 1992: Late Paleozoic kinematics of the Møre-Trøndelag Fault Zone and adjacent areas, central Norway. *Norsk Geologisk Tidsskrift 72*, 141-158.

Sherlock, S.C. 2001: Two-stage erosion and deposition in a continental margin setting: an $^{40}Ar/^{39}Ar$ laserprobe study of offshore detrital white micas in the Norwegian Sea. *Journal of the Geological Society, London 148*, 793-799.

Siedlecka, A. 1975: Old Red Sandstone lithostratigraphy and sedimentation of the Outer Fosen Area, Trondheim Region. *Norges geologiske undersøkelse 321*, 1-35.

Siedlecka, A. & Siedlecki, S. 1972: A contribution to the geology of the Downtonian sedimentary rocks of Hitra. *Norges geologiske undersøkelse 275*, 1-28.

Skilbrei, J.R, Olesen, O., Osmundsen, P.-T., Kihle, O., Aaro, S. & Fjellanger, E. 2002: A study of basement structures and some onshore-offshore correlations in Central Norway. *Norwegian Journal of Geology 82*, 263-279.

Sommaruga, A. & Bøe, R. 2002: Geometry and subcrop maps of shallow Jurassic basins along the Mid-Norway coast. *Marine and Petroleum Geology 19*, 1029-1042.

Steel, R.J. 1976: Devonian basins of western Norway—sedimentary response to tectonism and varying tectonic context. *Tectonophysics 36*, 207-224.

Terry, M.P., Robinson, P., Hamilton, M.A. & Jercinovic, M.J. 2000: Monazite geochronology of UHP and HP metamorphism, deformation, and exhumation, Nordøyane, Western Gneiss Region, Norway. *American Mineralogist 85*, 1651-1664.

Torsvik, T.H., Sturt, B.A., Ramsay, D.M., Kisch, H.J. & Bering, D. 1986: The tectonic implications of Solundian (Upper Devonian) magnetization of the Devonian rocks of Kvamshesten, western Norway. *Earth and Planetary Science Letters 80*, 337-347.

Torsvik, T.H., Sturt, B.A., Swensson, E., Andersen, T.B. & Dewey, J.F. 1992: Palaeomagnetic dating of fault rocks: evidence for Permian and Mesozoic movements and brittle deformation along the extensional Dalsfjord Fault, western Norway. *Geophysical Journal International 109*, 565-580.

Tucker, R.D., Bradley, D.C., Ver Straeten, C.A., Harris, A.G., Ebert, J.R. & McCutcheon, S.R. 1998: New U-Pb zircon ages and the duration and division of Devonian time. *Earth and Planetary Science Letters 158*, 175-186.

Turner, G., Huneke, J.C., Podosek, F.A. & Wasserburg, G.J. 1971: $^{40}Ar/^{39}Ar$ ages and cosmic ray exposure ages of Apollo 14 samples. *Earth and Planetary Science Letters 12*, 19-35.

Vogt, T. 1929: Den norske fjellkjedes revolusjons-historie. *Norsk Geologisk Tidsskrift 10*, 97-115.

Watts, L.M. 2001: The Walls Boundary Fault Zone and the Møre-Trøndelag Fault Complex: a case study of two reactivated fault zones. Unpublished Ph.D. thesis, University of Durham. 550 pp.

Whitham, A.G., Morton, A.C. & Fanning, C.M. 2004: Insights into Cretaceous-Palaeogene sediment transport paths and basin evolution in the North Atlantic from a heavy mineral study of sandstones from southern East Greenland. *Petroleum Geoscience 10*, 61-72.

## Table 1. $^{40}Ar/^{39}Ar$ data tables

| Temp (°C) | $^{40}Ar/^{39}Ar$ | $^{38}Ar/^{39}Ar$ | $^{37}Ar/^{39}Ar$ | $^{36}Ar/^{39}Ar$ | $^{39}Ar$ ($10^{-12}$ mol) | F$^{39}Ar$ | %$^{40}Ar^*$ | $^{40}Ar^*/^{39}Ar_K$ | Age (Ma) | ±1σ |
|---|---|---|---|---|---|---|---|---|---|---|
| **K-feldspar** | | | | | | | | | | |
| **6407/10-3 orthogneiss** | | | **J=.0043530** | **wt<3.0 mg** | | | | | | |
| 400 | 71.899 | 0.063 | 0.000 | 62.183 | 0.239 | 0.23 | 74.4 | 53.48 | 377.75 | 2.70 |
| 400 | 49.110 | 0.010 | 0.000 | 15.004 | 0.134 | 0.36 | 90.9 | 44.63 | 320.46 | 4.38 |
| 450 | 46.493 | 0.015 | 0.000 | 12.661 | 0.332 | 0.69 | 91.8 | 42.70 | 307.75 | 2.35 |
| 450 | 45.161 | 0.005 | 0.000 | 8.072 | 0.218 | 0.90 | 94.6 | 42.73 | 307.91 | 2.70 |
| 500 | 48.609 | 0.009 | 0.001 | 6.170 | 0.730 | 1.61 | 96.2 | 46.74 | 334.29 | 0.89 |
| 500 | 49.069 | 0.008 | 0.043 | 3.178 | 0.523 | 2.13 | 98.0 | 48.09 | 343.07 | 1.54 |
| 550 | 51.979 | 0.013 | 0.033 | 4.581 | 1.239 | 3.34 | 97.3 | 50.58 | 359.20 | 0.86 |
| 550 | 53.844 | 0.007 | 0.012 | 4.672 | 0.922 | 4.24 | 97.3 | 52.42 | 370.98 | 0.57 |
| 600 | 70.908 | 0.012 | 0.019 | 57.451 | 1.774 | 5.97 | 76.0 | 53.89 | 380.35 | 0.91 |
| 600 | 67.266 | 0.016 | 0.006 | 44.074 | 1.281 | 7.22 | 80.6 | 54.19 | 382.32 | 0.84 |
| 650 | 61.557 | 0.014 | 0.024 | 23.797 | 1.928 | 9.10 | 88.5 | 54.48 | 384.13 | 0.65 |
| 650 | 53.457 | 0.012 | 0.000 | 1.544 | 2.789 | 11.83 | 99.1 | 52.95 | 374.41 | 0.59 |
| 700 | 57.836 | 0.008 | 0.027 | 16.209 | 3.393 | 15.14 | 91.6 | 53.00 | 374.72 | 0.35 |
| 700 | 58.583 | 0.008 | 0.041 | 18.264 | 1.607 | 16.71 | 90.7 | 53.14 | 375.62 | 0.41 |
| 750 | 54.326 | 0.011 | 0.024 | 4.877 | 2.100 | 18.76 | 97.3 | 52.84 | 373.69 | 1.41 |
| 750 | 53.310 | 0.009 | 0.013 | 1.328 | 2.469 | 21.17 | 99.2 | 52.87 | 373.89 | 0.36 |
| 800 | 53.855 | 0.006 | 0.012 | 0.520 | 3.200 | 24.29 | 99.6 | 53.65 | 378.89 | 0.90 |
| 800 | 53.662 | 0.006 | 0.011 | 0.544 | 2.967 | 27.19 | 99.6 | 53.45 | 377.61 | 0.65 |
| 800 | 53.821 | 0.011 | 0.017 | 0.635 | 2.926 | 30.05 | 99.6 | 53.59 | 378.46 | 1.08 |
| 800 | 53.732 | 0.009 | 0.008 | 0.803 | 5.300 | 35.23 | 99.5 | 53.45 | 377.57 | 0.39 |
| 750 | 53.176 | 0.010 | 0.090 | 0.020 | 0.244 | 35.47 | 99.9 | 53.13 | 375.55 | 3.21 |
| 800 | 53.145 | 0.004 | 0.076 | 0.008 | 0.632 | 36.08 | 99.9 | 53.10 | 375.37 | 1.03 |
| 850 | 54.185 | 0.008 | 0.029 | 0.820 | 1.670 | 37.71 | 99.5 | 53.90 | 380.44 | 0.34 |
| 900 | 54.274 | 0.007 | 0.003 | 0.684 | 3.148 | 40.79 | 99.5 | 54.02 | 381.24 | 0.21 |
| 950 | 53.798 | 0.010 | 0.004 | 0.798 | 4.538 | 45.22 | 99.5 | 53.52 | 378.00 | 0.57 |
| 1000 | 53.571 | 0.006 | 0.012 | 0.932 | 5.460 | 50.55 | 99.4 | 53.25 | 376.30 | 0.52 |
| 1050 | 53.563 | 0.007 | 0.010 | 1.183 | 5.707 | 56.13 | 99.3 | 53.17 | 375.78 | 0.28 |
| 1075 | 53.334 | 0.005 | 0.009 | 1.135 | 4.959 | 60.97 | 99.3 | 52.95 | 374.40 | 0.20 |
| 1125 | 53.808 | 0.009 | 0.011 | 0.773 | 8.037 | 68.82 | 99.5 | 53.53 | 378.11 | 0.33 |
| 1200 | 53.182 | 0.009 | 0.012 | 1.057 | 7.313 | 75.97 | 99.3 | 52.82 | 373.58 | 0.53 |
| 1230 | 53.662 | 0.007 | 0.010 | 0.446 | 9.533 | 85.28 | 99.7 | 53.48 | 377.79 | 0.36 |
| 1260 | 53.737 | 0.009 | 0.010 | 0.545 | 9.518 | 94.58 | 99.6 | 53.53 | 378.09 | 0.49 |
| 1290 | 53.927 | 0.010 | 0.012 | 0.661 | 5.554 | 100 | 99.6 | 53.68 | 379.08 | 0.35 |

TFA = 375.8 ± 3.4 Ma WMA = 377.3 ± 3.4 Ma (steps 12-33, 90.9% $^{39}Ar$ gas)

| Temp (°C) | $^{40}Ar/^{39}Ar$ | $^{38}Ar/^{39}Ar$ | $^{37}Ar/^{39}Ar$ | $^{36}Ar/^{39}Ar$ | $^{39}Ar$ ($10^{-12}$ mol) | $F^{39}Ar$ | $\%^{40}Ar^*$ | $^{40}Ar^*/^{39}Ar_K$ | Age (Ma) | ±1σ |
|---|---|---|---|---|---|---|---|---|---|---|
| **biotite** | | | | | | | | | | |
| **6407/10-3 orthogneiss** | | | **J=.0043510** | **wt<3.0 mg** | | | | | | |
| 600 | 50.949 | 0.022 | 0.002 | 25.318 | 42.617 | 9.01 | 85.2 | 43.42 | 312.35 | 0.57 |
| 700 | 62.025 | 0.027 | 0.000 | 20.487 | 82.393 | 26.42 | 90.2 | 55.92 | 393.11 | 0.66 |
| 750 | 55.824 | 0.029 | 0.031 | 0.966 | 60.014 | 39.11 | 99.4 | 55.49 | 390.40 | 0.50 |
| 790 | 64.827 | 0.020 | 0.000 | 28.143 | 37.913 | 47.12 | 87.1 | 56.46 | 396.52 | 1.61 |
| 820 | 59.868 | 0.019 | 0.058 | 10.62 | 23.069 | 52.00 | 94.7 | 56.69 | 397.94 | 1.76 |
| 850 | 55.989 | 0.014 | 0.000 | 1.086 | 17.497 | 55.70 | 99.3 | 55.62 | 391.20 | 1.46 |
| 885 | 58.431 | 0.011 | 0.046 | 2.966 | 16.86 | 59.26 | 98.4 | 57.51 | 403.12 | 0.97 |
| 925 | 57.604 | 0.021 | 0.000 | 2.295 | 23.09 | 64.14 | 98.7 | 56.88 | 399.14 | 0.51 |
| 965 | 57.428 | 0.021 | 0.045 | 2.186 | 33.389 | 71.20 | 98.8 | 56.74 | 398.26 | 0.46 |
| 1000 | 55.972 | 0.018 | 0.025 | 0.852 | 42.231 | 80.12 | 99.5 | 55.67 | 391.55 | 1.69 |
| 1040 | 56.273 | 0.019 | 0.025 | 1.029 | 38.862 | 88.34 | 99.4 | 55.92 | 393.12 | 1.18 |
| 1080 | 55.764 | 0.016 | 0.045 | 1.287 | 30.312 | 94.74 | 99.2 | 55.34 | 389.43 | 0.49 |
| 1130 | 55.067 | 0.027 | 0.035 | 1.751 | 16.557 | 98.24 | 99.0 | 54.51 | 384.14 | 1.55 |
| 1200 | 53.848 | 0.018 | 0.296 | 2.406 | 8.314 | 100 | 98.7 | 53.12 | 375.33 | 2.09 |
| TFA = 385.9 ± 3.5 Ma WMA = 394.7 ± 3.5 Ma (steps 2-12, 85.7% $^{39}Ar$ gas) | | | | | | | | | | |
| **LYS10B** | | | | | | | | | | |
| **white mica, pegmatite clast** | | | **J=.0062780** | **wt=0.3 mg** | | | | | | |
| 529 | 71.545 | 0.023 | 35.504 | 136.669 | 0.014 | 0.10 | 49.0 | 35.02 | 358.75 | 33.03 |
| 608 | 69.924 | 0.000 | 131.418 | 64.488 | 0.014 | 0.19 | 100.8 | 70.47 | 661.20 | 35.87 |
| 665 | 66.090 | 0.009 | 19.422 | 116.971 | 0.050 | 0.54 | 50.8 | 33.59 | 345.43 | 8.62 |
| 710 | 383.239 | 0.093 | 17.764 | 1049.682 | 0.109 | 1.30 | 19.8 | 75.79 | 702.53 | 24.29 |
| 757 | 46.576 | 0.005 | 0.000 | 21.448 | 0.226 | 2.89 | 86.3 | 40.21 | 406.29 | 1.86 |
| 803 | 41.787 | 0.006 | 0.015 | 3.530 | 4.573 | 34.95 | 97.4 | 40.72 | 410.89 | 0.16 |
| 848 | 40.902 | 0.006 | 0.110 | 0.900 | 8.205 | 92.49 | 99.3 | 40.62 | 410.01 | 0.18 |
| 880 | 41.881 | 0.006 | 0.179 | 3.545 | 0.773 | 97.91 | 97.5 | 40.83 | 411.86 | 1.06 |
| 903 | 53.104 | 0.006 | 2.087 | 42.438 | 0.299 | 100 | 76.8 | 40.78 | 411.42 | 2.13 |
| TFA = 412.5 ± 3.6 Ma WMA = 410.2 ± 3.5 Ma (steps 5-9, 98.7% $^{39}Ar$ gas) | | | | | | | | | | |
| **LYS-11** | | | | | | | | | | |
| **biotite, marble clast** | | | **J=.0062850** | **wt=1.0 mg** | | | | | | |
| 524 | 110.864 | 0.075 | 31.281 | 300.716 | 0.069 | 0.16 | 22.6 | 25.05 | 263.95 | 28.35 |
| 575 | 13.447 | 0.022 | 12.765 | 28.068 | 0.248 | 0.72 | 45.4 | 6.11 | 68.01 | 5.43 |
| 601 | 11.431 | 0.014 | 10.010 | 13.216 | 0.429 | 1.69 | 72.6 | 8.29 | 91.73 | 3.26 |
| 659 | 28.732 | 0.013 | 8.667 | 37.410 | 0.277 | 2.32 | 64.2 | 18.44 | 197.91 | 4.67 |
| 706 | 195.699 | 0.074 | 7.765 | 479.698 | 0.261 | 2.91 | 28.1 | 54.94 | 535.44 | 11.09 |
| 754 | 53.073 | 0.018 | 5.950 | 20.401 | 0.489 | 4.02 | 90.0 | 47.75 | 473.76 | 3.67 |
| 786 | 48.833 | 0.018 | 4.308 | 12.341 | 0.500 | 5.15 | 93.5 | 45.68 | 455.59 | 1.97 |
| 829 | 45.163 | 0.015 | 0.000 | 11.477 | 0.678 | 6.68 | 92.4 | 41.74 | 420.54 | 1.12 |
| 873 | 41.693 | 0.017 | 0.000 | 3.189 | 1.243 | 9.50 | 97.7 | 40.72 | 411.34 | 0.68 |
| 899 | 40.136 | 0.016 | 0.000 | 1.681 | 2.387 | 14.91 | 98.7 | 39.61 | 401.27 | 0.39 |
| 950 | 40.397 | 0.018 | 0.000 | 1.967 | 4.551 | 25.22 | 98.5 | 39.79 | 402.88 | 0.20 |
| 990 | 40.284 | 0.017 | 0.000 | 1.868 | 8.093 | 43.55 | 98.6 | 39.70 | 402.11 | 0.55 |
| 1039 | 39.838 | 0.015 | 0.217 | 0.538 | 14.012 | 75.30 | 99.6 | 39.68 | 401.86 | 0.19 |
| 1100 | 40.328 | 0.020 | 0.047 | 1.243 | 10.902 | 100 | 99.0 | 39.94 | 404.24 | 0.31 |
| TFA = 399.2 ± 3.5 Ma WMA = 402.7 ± 3.5 Ma (steps 10-14, 90.5% $^{39}Ar$ gas) | | | | | | | | | | |

| Temp (°C) | $^{40}Ar/^{39}Ar$ | $^{38}Ar/^{39}Ar$ | $^{37}Ar/^{39}Ar$ | $^{36}Ar/^{39}Ar$ | $^{39}Ar$ ($10^{-12}$ mol) | $F^{39}Ar$ | $\%^{40}Ar^*$ | $^{40}Ar^*/^{39}Ar_K$ | Age (Ma) | ±1σ |
|---|---|---|---|---|---|---|---|---|---|---|
| **LYS 10A** | | | | | | | | | | |
| **K-feldspar, orthogneiss clast** | | | **J=.0059740** | **wt=2.8 mg** | | | | | | |
| 400 | 57.772 | 0.023 | 0.000 | 63.965 | 0.268 | 0.26 | 67.2 | 38.85 | 376.72 | 6.76 |
| 500 | 38.196 | 0.011 | 0.000 | 9.616 | 1.928 | 2.17 | 92.5 | 35.33 | 345.68 | 0.95 |
| 600 | 37.589 | 0.011 | 0.412 | 4.947 | 5.321 | 7.42 | 96.2 | 36.16 | 353.07 | 0.49 |
| 630 | 72.350 | 0.025 | 0.034 | 109.445 | 2.967 | 10.34 | 55.3 | 39.99 | 386.70 | 1.27 |
| 660 | 39.917 | 0.008 | 0.000 | 9.878 | 2.189 | 12.50 | 92.6 | 36.98 | 360.26 | 0.85 |
| 680 | 39.586 | 0.005 | 0.000 | 8.514 | 2.442 | 14.91 | 93.6 | 37.05 | 360.90 | 0.75 |
| 710 | 38.820 | 0.009 | 0.000 | 3.507 | 4.465 | 19.32 | 97.3 | 37.76 | 367.18 | 0.38 |
| 740 | 39.088 | 0.010 | 0.000 | 3.214 | 3.380 | 22.65 | 97.5 | 38.12 | 370.31 | 0.55 |
| 760 | 44.403 | 0.012 | 0.000 | 22.845 | 1.893 | 24.52 | 84.7 | 37.63 | 366.03 | 0.94 |
| 820 | 47.362 | 0.014 | 0.000 | 28.643 | 2.156 | 26.64 | 82.1 | 38.88 | 376.97 | 0.89 |
| 860 | 41.085 | 0.013 | 0.117 | 8.807 | 6.111 | 32.67 | 93.7 | 38.48 | 373.47 | 0.37 |
| 900 | 38.932 | 0.007 | 0.000 | 4.779 | 9.685 | 42.22 | 96.3 | 37.50 | 364.86 | 0.34 |
| 930 | 39.064 | 0.008 | 0.000 | 4.358 | 11.338 | 53.41 | 96.6 | 37.75 | 367.11 | 0.35 |
| 950 | 39.484 | 0.009 | 0.000 | 4.716 | 9.316 | 62.60 | 96.4 | 38.07 | 369.89 | 0.31 |
| 970 | 40.511 | 0.011 | 0.000 | 6.387 | 8.303 | 70.79 | 95.3 | 38.60 | 374.56 | 0.28 |
| 1000 | 40.865 | 0.010 | 0.000 | 7.750 | 5.290 | 76.01 | 94.3 | 38.55 | 374.13 | 0.40 |
| 1020 | 41.707 | 0.008 | 0.022 | 15.971 | 2.295 | 78.27 | 88.6 | 36.97 | 360.20 | 0.49 |
| 1060 | 41.972 | 0.011 | 0.000 | 16.778 | 2.097 | 80.34 | 88.1 | 36.99 | 360.40 | 0.96 |
| 1100 | 42.195 | 0.011 | 0.163 | 14.664 | 2.512 | 82.82 | 89.7 | 37.86 | 368.08 | 0.83 |
| 1160 | 40.417 | 0.011 | 0.078 | 7.272 | 5.261 | 88.01 | 94.7 | 38.26 | 371.54 | 0.38 |
| 1220 | 40.014 | 0.009 | 0.110 | 5.134 | 12.159 | 100 | 96.2 | 38.49 | 373.59 | 0.25 |

TFA = 368.5 ± 3.2 Ma WMA = 371.0 ± 3.2 Ma (steps 7-21, 85.1% $^{39}Ar$ gas)

| Laser shot ID | $^{40}Ar/^{39}Ar$ | $^{38}Ar/^{39}Ar$ | $^{37}Ar/^{39}Ar$ | $^{36}Ar/^{39}Ar$ | $^{39}Ar$ ($10^{-12}$ mol) | $F^{39}Ar$ | $\%^{40}Ar^*$ | $^{40}Ar^*/^{39}Ar_K$ | Age (Ma) | ±1σ |
|---|---|---|---|---|---|---|---|---|---|---|
| **LYS-9** | | | | | | | | | | |
| **white mica, red sandstone** | | | **J=.0062850** | | | | | | | |
| 8462 | 39.612 | 0.006 | 0.656 | 0.400 | 0.489 | 3.58 | 99.8 | 39.54 | 400.64 | 1.55 |
| 8463 | 38.943 | 0.008 | 1.854 | 2.277 | 0.623 | 8.14 | 98.7 | 38.45 | 390.72 | 0.85 |
| 8468 | 38.723 | 0.009 | 0.196 | 0.147 | 0.999 | 15.46 | 99.9 | 38.67 | 392.73 | 0.55 |
| 8469 | 39.345 | 0.007 | 0.667 | 2.002 | 0.586 | 19.76 | 98.6 | 38.80 | 393.90 | 0.94 |
| 8470 | 38.067 | 0.006 | 0.425 | 0.637 | 0.844 | 25.94 | 99.6 | 37.90 | 385.65 | 1.34 |
| 8471 | 38.914 | 0.008 | 2.458 | 0.291 | 0.504 | 29.63 | 100.4 | 39.08 | 396.45 | 1.17 |
| 8472 | 39.019 | 0.008 | 0.385 | 0.448 | 0.764 | 35.23 | 99.7 | 38.90 | 394.82 | 0.80 |
| 8474 | 39.526 | 0.007 | 0.000 | 0.527 | 0.929 | 42.03 | 99.5 | 39.34 | 398.82 | 0.74 |
| 8475 | 38.770 | 0.006 | 0.157 | 0.282 | 1.041 | 49.65 | 99.8 | 38.68 | 392.76 | 0.46 |
| 8476 | 40.964 | 0.007 | 0.244 | 0.099 | 1.477 | 60.47 | 99.9 | 40.93 | 413.26 | 0.49 |
| 8480 | 39.090 | 0.004 | 0.000 | 1.483 | 0.957 | 67.47 | 98.8 | 38.62 | 392.28 | 0.87 |
| 8481 | 39.928 | 0.009 | 0.000 | 1.543 | 1.300 | 76.99 | 98.8 | 39.44 | 399.76 | 0.37 |
| 8482 | 39.273 | 0.005 | 0.000 | 1.563 | 1.315 | 86.62 | 98.8 | 38.78 | 393.74 | 0.68 |
| 8483 | 39.525 | 0.009 | 0.000 | 1.263 | 0.814 | 92.58 | 99.0 | 39.12 | 396.84 | 1.15 |
| 8484 | 38.570 | 0.006 | 0.000 | 1.400 | 1.013 | 100 | 98.9 | 38.13 | 387.75 | 0.59 |
| 4440 | 43.010 | 0.001 | 0.056 | 1.098 | 1.426 | 15.52 | 99.2 | 42.67 | 410.86 | 0.39 |
| 4441 | 43.390 | 0.002 | 0.248 | 0.440 | 0.667 | 22.78 | 99.7 | 43.28 | 416.05 | 4.05 |
| 4443 | 41.982 | 0.000 | 0.060 | 0.889 | 1.046 | 34.16 | 99.3 | 41.71 | 402.53 | 1.71 |
| 4446 | 41.518 | 0.000 | 0.000 | 0.949 | 0.928 | 44.26 | 99.3 | 41.22 | 398.28 | 0.81 |

| Laser shot ID | $^{40}Ar/^{39}Ar$ | $^{38}Ar/^{39}Ar$ | $^{37}Ar/^{39}Ar$ | $^{36}Ar/^{39}Ar$ | $^{39}Ar$ ($10^{-12}$ mol) | $F^{39}Ar$ | $\%^{40}Ar^*$ | $^{40}Ar^*/^{39}Ar_K$ | Age (Ma) | ±1σ |
|---|---|---|---|---|---|---|---|---|---|---|
| 4447 | 41.322 | 0.001 | 0.000 | 2.072 | 0.496 | 49.65 | 98.5 | 40.69 | 393.70 | 1.18 |
| 4449 | 40.685 | 0.002 | 0.000 | 1.592 | 0.984 | 60.36 | 98.8 | 40.19 | 389.39 | 0.33 |
| 4450 | 41.182 | 0.000 | 0.000 | 0.013 | 0.373 | 64.42 | 99.9 | 41.16 | 397.76 | 0.65 |
| 4451 | 41.653 | 0.001 | 0.000 | 1.041 | 0.987 | 75.15 | 99.2 | 41.32 | 399.22 | 1.08 |
| 4453 | 40.902 | 0.000 | 0.000 | 0.159 | 1.229 | 88.52 | 99.8 | 40.83 | 394.96 | 0.49 |
| 4456 | 42.078 | 0.002 | 0.000 | 1.469 | 0.666 | 95.77 | 98.9 | 41.62 | 401.80 | 0.65 |
| 4457 | 41.064 | 0.000 | 0.000 | 0.013 | 0.389 | 100 | 99.9 | 41.04 | 396.74 | 1.12 |

*All ages cited at 1σ uncertainty; total fusion ages (TFA) and weighted mean ages (WMA) cited at 1σ including the uncertainty in J-value (1%). The total number of steps and their cumulative $^{39}Ar$ gas as % of total gas released in the experiment are noted. Data for all samples except LYS-9 were collected using resistance-furnace step-heating; data for single, detrital white mica grains of LYS-9 were obtained by fusion with a $CO_2$ laser operating at infrared wavelengths. No TFA or WMA is cited for the single-grain laser fusion analyses of LYS-9 (detrital white mica). See also Figure 4 and Table 2.*

## Table 2. $^{40}Ar/^{39}Ar$ data data summary for resistance-furnace step-heating samples

| Sample | Mineral | Rock | Total fusion age (Ma) | Weighted mean age (Ma) | Steps used | Inverse isochron age (Ma) | $^{40}Ar/^{36}Ar$ intercept | SUMS/ (n-2) |
|---|---|---|---|---|---|---|---|---|
| 6407/10-3 | K-feldspar | orthogneiss | 375.8±3.4 | **377.3±3.4** | 12-33 | 377.1±3.5 | 302.6±10.2 | 29.0 |
| 6407/10-3 | biotite | orthogneiss | 385.9±3.5 | 394.7±3.5 | 2-12 | 394.4±3.9 | 310.9±32.9 | 28.0 |
| LYS-10B | white mica | granite pegmatite (clast) | 412.5±3.6 | **410.2±3.5** | 5-9 | 410.4±3.6 | 301.7±10.9 | 4.1 |
| LYS-11 | biotite | marble(clast) | 399.2±3.5 | 402.7±3.5 | 10-14 | 401.6±3.6 | 374.2±72.1 | 7.7 |
| LYS-10A | K-feldspar | orthogneiss (clast) | 368.5±3.2 | 371.0±3.2 | 7-21 | 370.3±3.9 | 293.6±29.3 | 75.2 |

*All ages are cited at 1σ with 1% error in J-value included. Uncertainties for isochron ages are standard errors. Ages in bold are those preferred in the data interpretations and discussion. Age in italics (biotite from the well) is interpreted as a maximum age.*

# Appendix 1

## Analytical procedures, Geological Survey of Norway $^{40}Ar/^{39}Ar$ Geochronology Laboratory

Mineral separates were obtained using standard techniques. Before packing in Al-foil, mineral separates were hand-picked under a binocular microscope and rinsed in alternating acetone and distilled water. The sample packets (biotite and K-feldspar) from the offshore orthogneiss were stacked and irradiated together with monitor minerals at the Risø Nuclear Reactor, Roskilde, Denmark. Sample packets for LYS-10A K-feldspar, LYS-9 detrital white mica, LYS-10B white mica and LYS-11 biotite were stacked and loaded in sealed Al-capsules for irradiation in the 5C site at the McMaster Nuclear Reactor facility, Hamilton, Canada (the McMaster samples were irradiated in two different batches). The samples at McMaster were irradiated for 25 hours (50 MWH) with nominal neutron flux of 4 x 10e13 $n/cm^2/s$; nominal temperature in the irradiation site is <50˚C (M. Butler, pers. comm.). Production of isotopes from Ca and K were determined by irradiation of CaF and $K_2SO_4$ salts; values of 36/37Ca = 0.00035, 39/37Ca = 0.0011, and 40/39K = 0.022 were used for the McMaster samples LYS-9 and LYS-10B; values of 36/37Ca = 0.000238, 39/37Ca = 0.001121, and 40/39K = 0.02878 were used for the McMaster samples LYS-10A and LYS-11 and a second batch of LYS-9 micas; values of 36/37Ca = 0.000255, 39/37Ca = 0.00067, and 40/39K = 0.048 were used for the Risø irradiation. Neutron fluence monitors included Taylor Creek Rhyolite sanidine, Tinto biotite and Hb3gr hornblende with ages of 27.92 Ma (TCR; Duffield & Dalrymple 1990), 410.3 Ma (Tinto; Rex & Guise 1995) and 1072 ± 11 Ma (Hb3gr; Turner et al. 1971). Uncertainty in J-values for monitors in both irradiations ranged from 0.1 to 1.0 % without including error in monitor age; we incorporated a conservative 1% error in J-value for all unknowns.

Samples were analyzed at the $^{40}Ar/^{39}Ar$ Geochronology Laboratory at the Norwegian Geological Survey. Gas from irradiated samples was released in a step-wise fashion from a resistance furnace (offshore core samples and samples LYS-10A, LYS-10B and LYS-11) or via heating with a 20W $CO_2$ laser (Merchantek Laser Ablation Station) operating at infrared (IR) wavelengths (LYS-9 white mica). The $CO_2$ laser port is ZnS; the vacuum on the port window is maintained by an external, mechanical (rotary) pump attached to the port flange. The laser chamber itself is maintained at high vacuum by a coupled turbo and rotary pump system. Samples in the laser ports were loaded in holes machined in aluminum pans. Laser operating conditions varied between 6-8 Hz, and 4-10% operating power (typically yielding 0.2-0.8 W at fusion). Furnace conditions are similar to those described in Eide et al. (2002).

Gas released from a sample at a single temperature step or laser shot was cleaned in the extraction line for 11 minutes using two pairs of SAES AP-10 getters, mounted in isolated sections of the line, each maintained with their own vacuum pumps. The purified gas was then analyzed on a MAP 215-50 mass spectrometer. Data for blanks, monitors and unknowns were collected on a Johnson electron multiplier with gain setting at 1, while the magnet was automatically scanned over masses 35 through 41 in a cycled, 'peak-hop' mode. Masses 37 through 40 were each measured in eight cycles and 10 counts per mass per cycle; mass 36 was measured with 20 counts per cycle.

Dynamic blank measurements on mass 40 indicate a stable background ($2.19 \times 10^{-14}$ ccSTP). Background levels (blanks) for the furnace were measured at 100 to 200˚C temperature increments prior to each sample analysis. Furnace blanks for biotite and K-feldspar from the offshore core were maintained at levels of 6-9 $\times 10^{-12}$ ccSTP for mass 40 and 7-9 $\times 10^{-14}$ ccSTP for mass 36 at temperatures of 500 through 1000˚C; blanks increased to 1-9 $\times 10^{-11}$ ccSTP for mass 40 and 1-3 $\times 10^{-13}$ ccSTP for mass 36 at high temperatures (1200-1400˚C). Furnace blanks for LYS-10A K-feldspar, LYS-10B white mica and LYS-11 biotite were slighly higher ($1.5 \times 10^{-11}$ to $1 \times 10^{-10}$ ccSTP for mass 40 at 500-1400oC; $9 \times 10^{-13}$ to $6.6 \times 10^{-14}$ ccSTP for mass 36 at 500-1400˚C). Background levels of masses 37 and 39 did not change signficantly from dynamic blank levels at any temperature ($2.1 \times 10^{-13}$ ccSTP for mass 37; $<3.3 \times 10^{-14}$ ccSTP for mass 39). Background levels for mass 38 were $1 \times 10^{-13}$ ccSTP at high temperatures and $<9 \times 10^{-14}$ ccSTP at temperatures < 1000˚C. At experimental temperatures between 600 and 1000˚C, furnace blanks for mass 40 were usually <1% of the sample signal size. Background levels for the laser port were measured every third to fourth sample measurement and were consistently maintained at 1.6-2.8 $\times 10^{-12}$ ccSTP for mass 40 and $2.2 \times 10^{-14}$ ccSTP for mass 36. Levels for masses 37, 38 and 39 were maintained at dynamic blank levels.

Data from unknowns were corrected for blanks prior to being reduced with the IAAA (Interactive Ar-Ar Analysis) software package (Visual Basic programming for PC Windows) written by T.H. Torsvik and N.O. Arnaud and based in part on equations in Dalrymple et al. (1981) and McDougall & Harrison (1999). Data reduction in IAAA incorporates corrections for interfering isotopes, mass discrimination (measured with an air pipette), error in blanks and decay of $^{37}Ar$.

# Det er her vi finner fremtidens energikilder:

# I det åpne sinn.

Kanskje vil det være vinden. Kanskje bølgene. Eller kanskje noe helt annet som ingen ennå har tenkt på. Det eneste som er helt sikkert er at et livskraftig samfunn er avhengig av en stabil energiforsyning. Derfor jobber vi i Hydro hele tiden med løsninger for å sikre fremtidige energibehov. Med 36.000 medarbeidere og virksomhet i nær 40 land er vi en ledende produsent av olje og gass til havs, verdens tredje største integrerte leverandør av aluminium og en pionér i fornybar energi og energieffektive løsninger. På terskelen til de neste 100 år bygger vi videre på vår evne til å skape livskraft for kunder, partnere og samfunnet som helhet. I 2005 fyller vi 100 år.

HYDRO

Progress of a different nature

www.hydro.com